

## Chopper-Stabilized, Two Wire Hall-Effect Latch

### FEATURES AND BENEFITS

- High speed, 4-phase chopper stabilization
  - Low switchpoint drift throughout temperature range
  - Low sensitivity to thermal and mechanical stresses
- On-chip protection
  - Supply transient protection
  - Reverse battery protection
- On-board voltage regulator
  - 3.0 to 24 V operation
- Solid-state reliability
- Industry leading ISO 7637-2 performance through use of proprietary, 40 V clamping structures

### DESCRIPTION

The A1245 is a two-wire Hall-effect latch. The device is produced on the Allegro™ advanced BiCMOS wafer fabrication process, which implements a patented high frequency, 4-phase, chopper-stabilization technique. This technique achieves magnetic stability over the full operating temperature range, and eliminates offsets inherent in devices with a single Hall element that are exposed to harsh application environments.

Two-wire latches are particularly advantageous in cost-sensitive applications because they require one less wire for operation versus the more traditional open-collector output switches. Additionally, the system designer inherently gains diagnostics because there is always output current flowing, which should be in either of two narrow ranges. Any current level not within these ranges indicates a fault condition.

The Hall-effect latch will be in the high output current state in the presence of a magnetic south polarity field of sufficient magnitude and will remain in this state until a sufficient north polarity field is present.

The device is offered in two package styles. The LH is a SOT-23W style, miniature low profile package for surface-mount applications. The UA is a 3-pin ultra-mini single inline packages (SIP) for through-hole mounting. Both packages are lead (Pb) free, with 100% matte tin leadframe plating.

### PACKAGES:

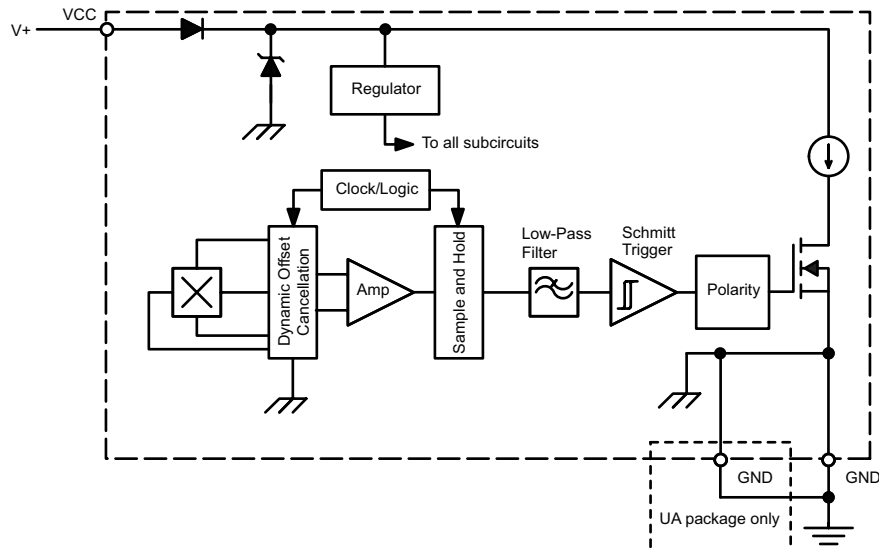
Not to scale



**3-pin ultramini SIP**  
1.5 × 4 × 3 mm  
(suffix UA)



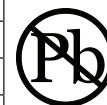
**3-pin SOT23-W**  
2 × 3 × 1 mm  
(suffix LH)



**Functional Block Diagram**

### Selection Guide

Part Number	Packing*	Package	Operating Ambient Temperature, $T_A$ (°C)	Supply Current at $I_{CC(L)}$ (mA)
A1245LLHLX-I1-T	13-in. reel, 10000 pieces/reel	3-pin SOT23W surface mount	-40 to 150	5 to 6.9
A1245LLHLX-I2-T	13-in. reel, 10000 pieces/reel	3-pin SOT23W surface mount	-40 to 150	2 to 5
A1245LUA-I1-T	Bulk, 500 pieces/bag	3-pin SIP through hole	-40 to 150	5 to 6.9
A1245LUA-I2-T	Bulk, 500 pieces/bag	3-pin SIP through hole	-40 to 150	2 to 5



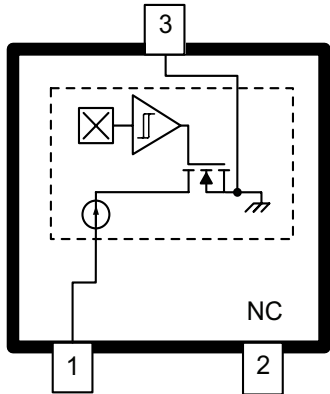
\*Contact Allegro for additional packing options

## SPECIFICATIONS

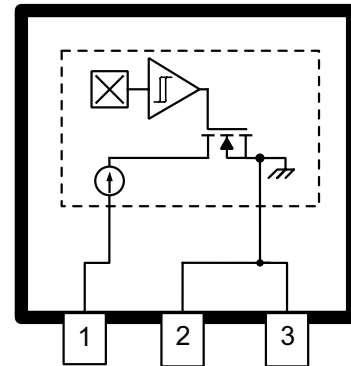
### Absolute Maximum Ratings

Characteristic	Symbol	Notes	Rating	Unit
Forward Supply Voltage	$V_{CC}$		28	V
Reverse Supply Voltage	$V_{RCC}$		-18	V
Magnetic Flux Density	B		Unlimited	G
Operating Ambient Temperature	$T_A$	Range L	-40 to 150	°C
Maximum Junction Temperature	$T_J(\max)$		165	°C
Storage Temperature	$T_{stg}$		-65 to 170	°C

### Pin-out Diagrams and Terminal List Table



**LH Package, 3-pin  
SOT23W Pin-out**



**UA Package, 3-pin SIP  
Pin-out**

### Terminal List Table

Name	Number		Function
	LH	UA	
VCC	1	1	Connects power supply to chip
NC	2	N/A	No connection (tie to GND; improved thermal characteristics) or float
GND	3	2, 3	Ground (Tie both to GND for improved thermal characteristics, or float unused GND pin)

**ELECTRICAL CHARACTERISTICS:** valid at  $T_A = -40^\circ\text{C}$  to  $150^\circ\text{C}$ ;  $T_J < T_{J(\text{max})}$ ; for LH and UA:  $C_{\text{BYP}} = 0.01 \mu\text{F}$ ; through operating supply voltage range; unless otherwise noted

Characteristics	Symbol	Test Conditions	Min.	Typ.	Max.	Unit
Supply Voltage <sup>1,2</sup>	$V_{\text{CC}}$	Operating	3.0	–	24	V
Supply Current	$I_{\text{CC(L)}}$	-I1   $B < B_{\text{RP}}$	5	–	6.9	mA
		-I2   $B < B_{\text{RP}}$	2	–	5	mA
	$I_{\text{CC(H)}}$	$B > B_{\text{OP}}$	12	–	17	mA
Supply Zener Clamp Voltage	$V_{\text{Z(sup)}}$	$I_{\text{CC(L)}}(\text{max}) + 3 \text{ mA}$ , $T_A = 25^\circ\text{C}$	28	–	–	V
Supply Zener Clamp Current	$I_{\text{Z(sup)}}$	$V_{\text{Z(sup)}} = 28 \text{ V}$	–	–	$I_{\text{CC(L)}}(\text{max}) + 3 \text{ mA}$	mA
Reverse Supply Current	$I_{\text{RCC}}$	$V_{\text{RCC}} = -18 \text{ V}$	–	–	-1.6	mA
Output Slew Rate <sup>3</sup>	$dl/dt$	No external bypass capacitor, capacitance of probe $C_S = 20 \text{ pF}$	–	90	–	mA/ $\mu\text{s}$
Chopping Frequency <sup>5</sup>	$f_c$		–	700	–	kHz
Power-Up Time <sup>2,4,5</sup>	$t_{\text{on}}$	$V_{\text{CC}} \geq V_{\text{CC}(\text{min})}$	–	–	25	$\mu\text{s}$
Power-Up State <sup>4,6,7</sup>	POS	$t_{\text{on}} < t_{\text{on}}(\text{max})$ , $V_{\text{CC}}$ slew rate $> 25 \text{ mV}/\mu\text{s}$	–	$I_{\text{CC(H)}}$	–	–

<sup>1</sup>  $V_{\text{CC}}$  represents the generated voltage between the VCC pin and the GND pin.

<sup>2</sup> The  $V_{\text{CC}}$  slew rate must exceed 600 mV/ms from 0 to  $V_{\text{CC}(\text{min})}$ . A slower slew rate through this range can affect device performance.

<sup>3</sup> Measured without bypass capacitor between VCC and GND. Use of a bypass capacitor results in slower current change.

<sup>4</sup> Power-Up Time is measured with and without an external bypass capacitor of 0.01  $\mu\text{F}$ ,  $B < B_{\text{RP}} - 10 \text{ G}$ . Adding a larger bypass capacitor would cause longer Power-Up Time.

<sup>5</sup> Guaranteed by characterization and design.

<sup>6</sup> Power-Up State as defined is true only with a  $V_{\text{CC}}$  slew rate of 25 mV/ $\mu\text{s}$  or greater.

<sup>7</sup> Power-Up State is defined during the power-on phase ( $t < t_{\text{ON}}$ ) until the device has fully powered-on ( $t_{\text{ON}}$ ), after which the output will correspond to the magnetic field level seen by the sensor. For  $t > t_{\text{on}}$  and  $B_{\text{RP}} < B < B_{\text{OP}}$ , Power-Up State is not defined.

**MAGNETIC CHARACTERISTICS<sup>1</sup>:** valid at  $T_A = -40^\circ\text{C}$  to  $150^\circ\text{C}$ ;  $T_J < T_{J(\text{max})}$ ; for LH and UA:  $C_{\text{BYP}} = 0.01 \mu\text{F}$ ; through operating supply voltage range; unless otherwise noted

Characteristics	Symbol	Test Conditions	Min.	Typ.	Max.	Unit <sup>2</sup>
Magnetic Operating Point	$B_{\text{OP}}$		5	–	40	G
Magnetic Release Point	$B_{\text{RP}}$		-40	–	-5	G
Hysteresis	$B_{\text{HYS}}$	$B_{\text{OP}} - B_{\text{RP}}$	15	40	65	G

<sup>1</sup> Relative values of B use the algebraic convention, where positive values indicate south magnetic polarity, and negative values indicate north magnetic polarity; therefore greater B values indicate a stronger south polarity field (or a weaker north polarity field, if present).

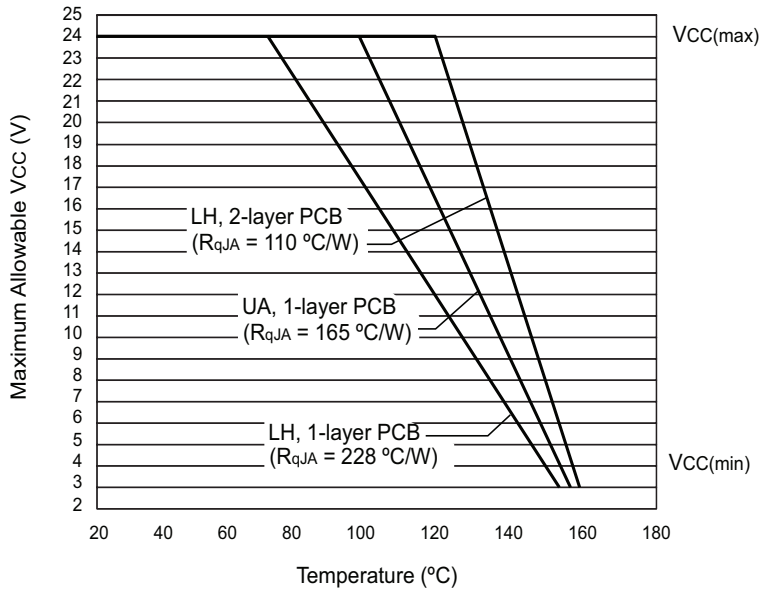
<sup>2</sup> 1 G (gauss) = 0.1 mT (millitesla).

**THERMAL CHARACTERISTICS** may require derating at maximum conditions, see application information

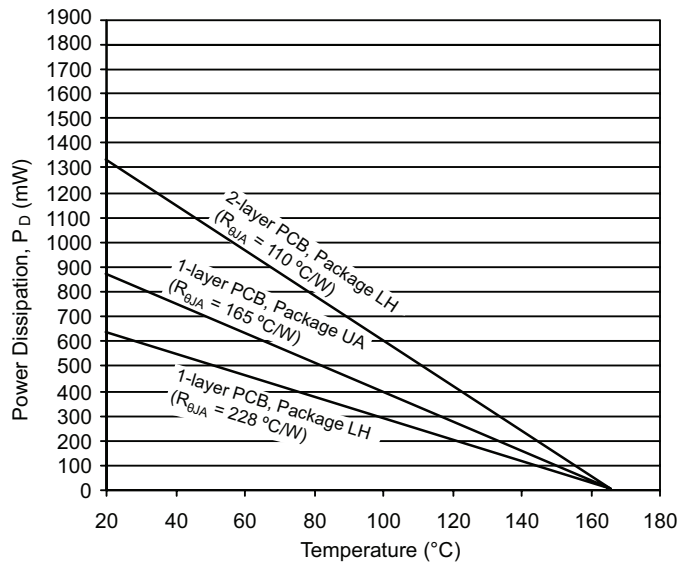
Characteristic	Symbol	Test Conditions*	Value	Units
Package Thermal Resistance	$R_{\theta JA}$	Package LH, 1-layer PCB with copper limited to solder pads	228	$^{\circ}\text{C}/\text{W}$
		Package LH, 2-layer PCB with 0.463 in. <sup>2</sup> of copper area each side connected by thermal vias	110	$^{\circ}\text{C}/\text{W}$
		Package UA, 1-layer PCB with copper limited to solder pads	165	$^{\circ}\text{C}/\text{W}$

\*Additional thermal information available on Allegro Web site.

**Power Derating Curve**

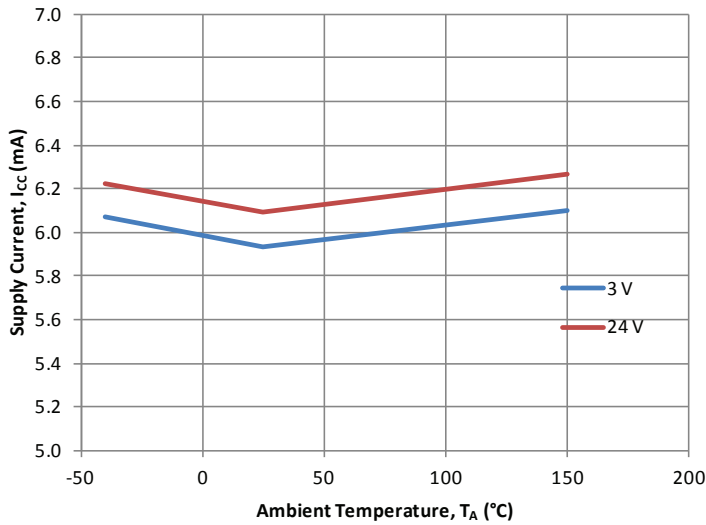


**Maximum Power Dissipation versus Ambient Temperature**

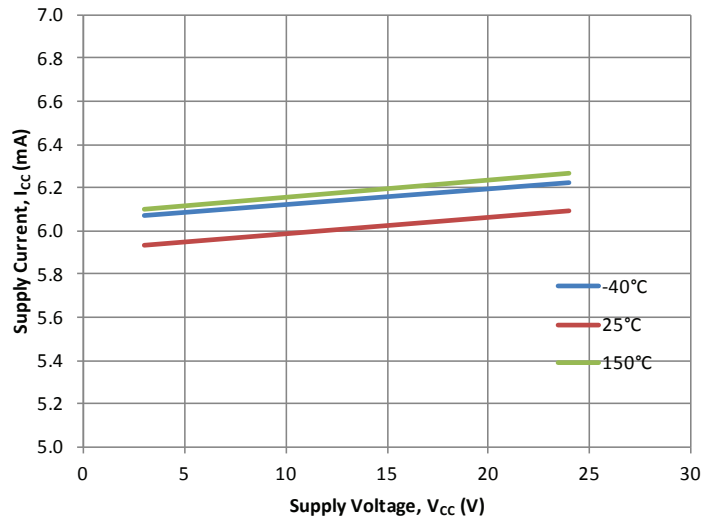


## CHARACTERISTIC PERFORMANCE

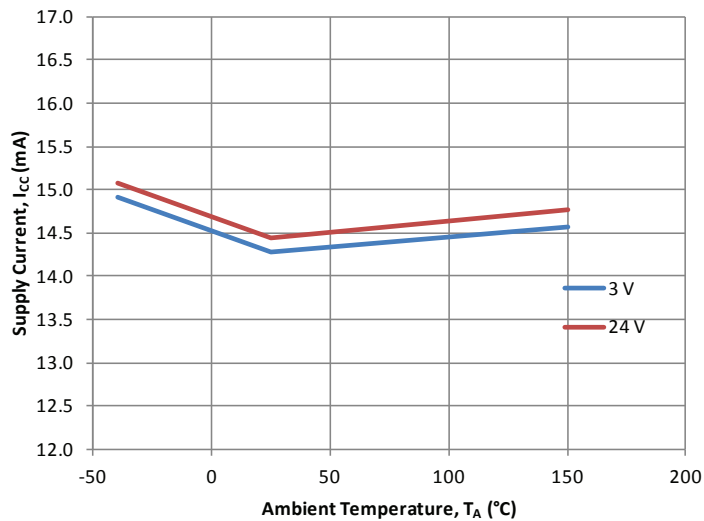
Average Supply Current (Low) vs. Temperature



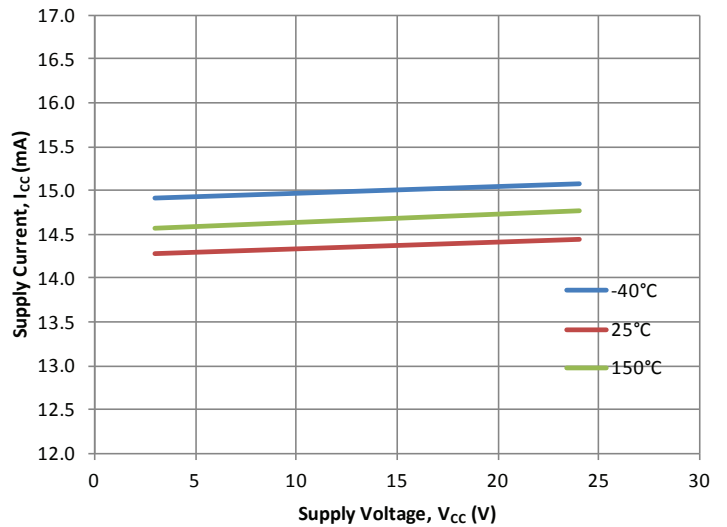
Average Supply Current (Low) vs. Supply Voltage



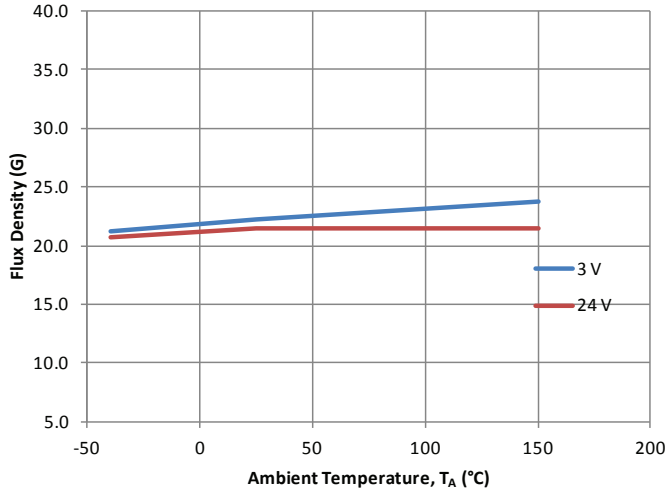
Average Supply Current (High) vs. Temperature



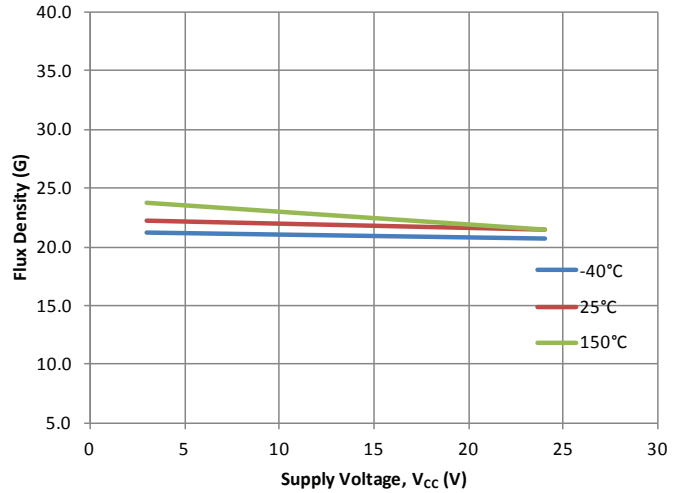
Average Supply Current (High) vs. Supply Voltage



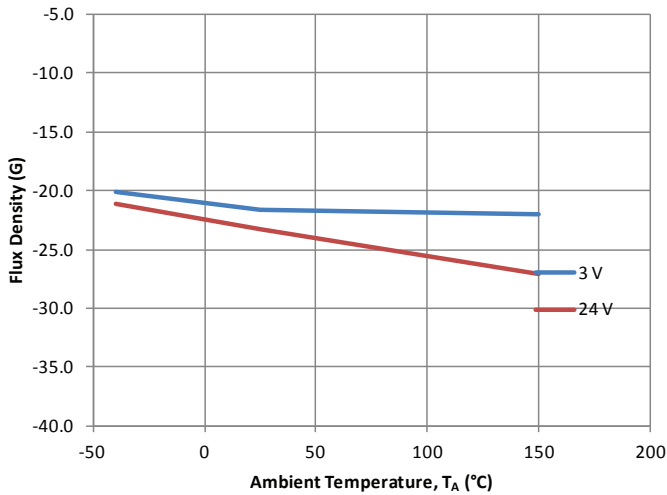
**Average  $B_{OP}$  vs. Temperature**



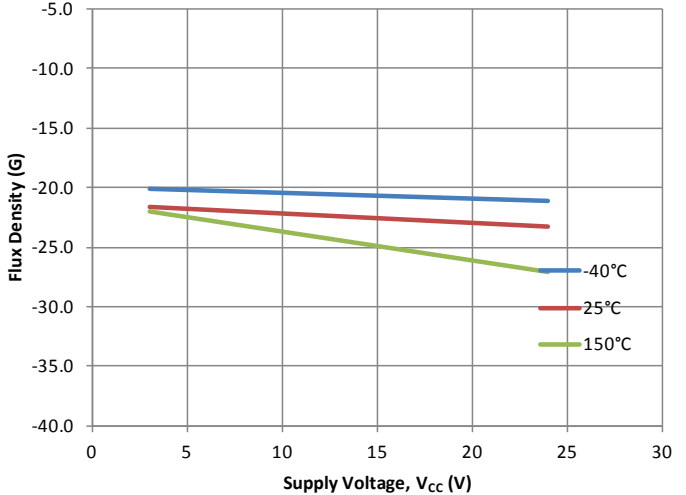
**Average  $B_{OP}$  vs. Supply Voltage**



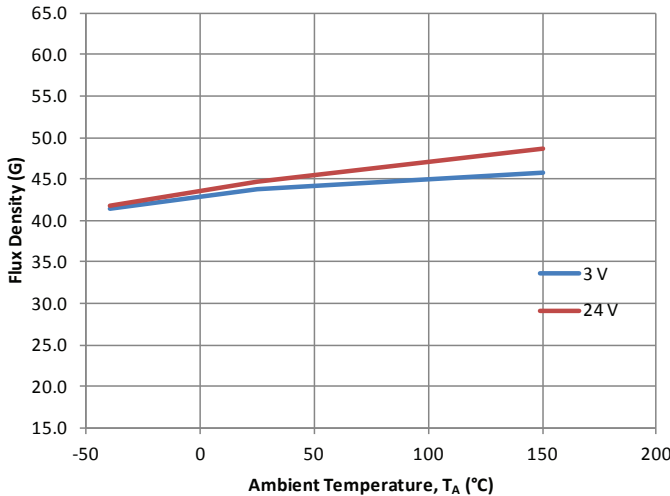
**Average  $B_{RP}$  vs. Temperature**



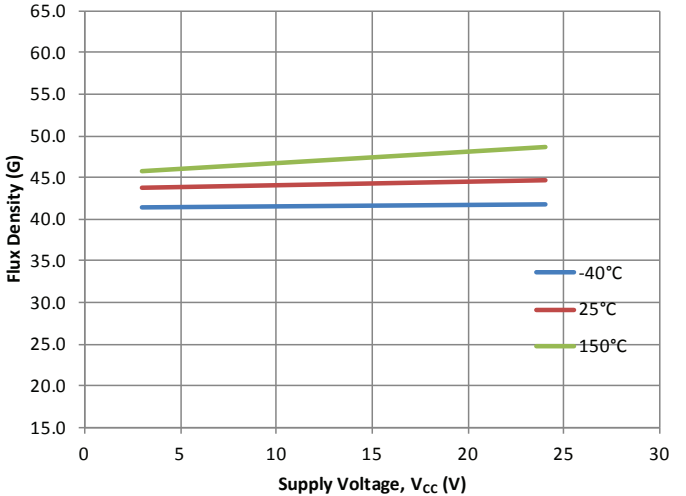
**Average  $B_{RP}$  vs. Supply Voltage**



**Average  $B_{HYS}$  vs. Temperature**



**Average  $B_{HYS}$  vs. Supply Voltage**



## FUNCTIONAL DESCRIPTION

The A1245 output,  $I_{CC}$ , switches high after the magnetic field at the Hall sensor IC exceeds the operate point threshold,  $B_{OP}$ . When the magnetic field is reduced to below the release point threshold,  $B_{RP}$ , the device output goes low. This is shown in Figure 1.

The difference between the magnetic operate and release points is called the hysteresis of the device,  $B_{HYS}$ . This built-in hysteresis allows clean switching of the output even in the presence of external mechanical vibration and electrical noise.

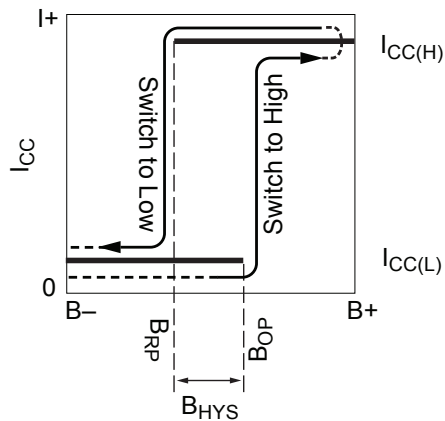


**Figure 1: Hysteresis for the A1245**

On the horizontal axis, the B+ direction indicates increasing south polarity magnetic field strength, and the B- direction indicates decreasing south polarity field strength (including the case of increasing north polarity).

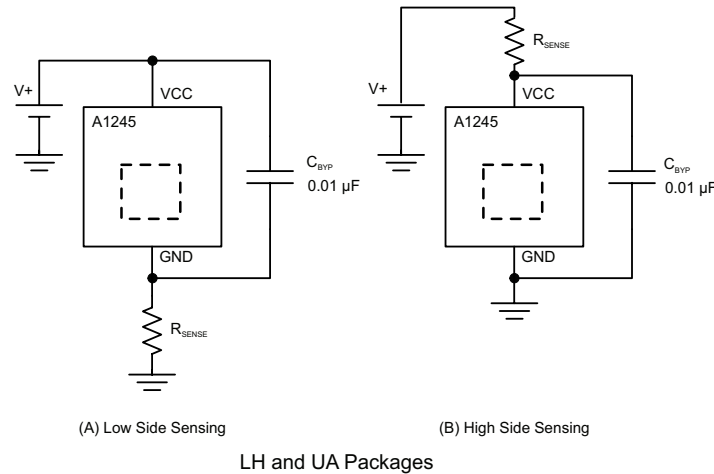


**Figure 2: Typical Application Circuits**

## Chopper Stabilization Technique

When using Hall-effect technology, a limiting factor for switchpoint accuracy is the small signal voltage developed across the Hall element. This voltage is disproportionately small relative to the offset that can be produced at the output of the Hall sensor IC. This makes it difficult to process the signal while maintaining an accurate, reliable output over the specified operating temperature and voltage ranges. Chopper stabilization is a unique approach used to minimize Hall offset on the chip. The patented Allegro technique, namely Dynamic Quadrature Offset Cancellation, removes key sources of the output drift induced by thermal and mechanical stresses. This offset reduction technique is based on a signal modulation-demodulation process. The undesired offset signal is separated from the magnetic field-induced signal in the frequency domain, through modulation. The subsequent demodulation acts as a modulation process for the offset, causing the magnetic field-induced signal to recover

its original spectrum at base band, while the DC offset becomes a high-frequency signal. The magnetic-sourced signal then can pass through a low-pass filter, while the modulated DC offset is suppressed. The chopper stabilization technique uses a 350 kHz high frequency clock. For demodulation process, a sample and hold technique is used, where the sampling is performed at twice the chopper frequency. This high-frequency operation allows a greater sampling rate, which results in higher accuracy and faster signal-processing capability. This approach desensitizes the chip to the effects of thermal and mechanical stresses, and produces devices that have extremely stable quiescent Hall output voltages and precise recoverability after temperature cycling. This technique is made possible through the use of a BiCMOS process, which allows the use of low-offset, low-noise amplifiers in combination with high-density logic integration and sample-and-hold circuits.

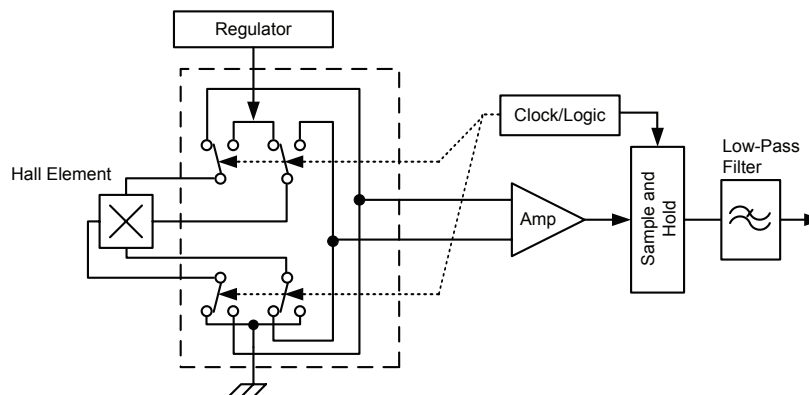


**Figure 3: Chopper Stabilization Circuit (Dynamic Quadrature Offset Cancellation)**

## Power Derating

The device must be operated below the maximum junction temperature of the device,  $T_J(\max)$ . Under certain combinations of peak conditions, reliable operation may require derating supplied power or improving the heat dissipation properties of the application. This section presents a procedure for correlating factors affecting operating  $T_J$ . (Thermal data is also available on the Allegro MicroSystems Web site.)

The Package Thermal Resistance,  $R_{\theta JA}$ , is a figure of merit summarizing the ability of the application and the device to dissipate heat from the junction (die), through all paths to the ambient air. Its primary component is the Effective Thermal Conductivity,  $K$ , of the printed circuit board, including adjacent devices and traces. Radiation from the die through the device case,  $R_{\theta JC}$ , is relatively small component of  $R_{\theta JA}$ . Ambient air temperature,  $T_A$ , and air motion are significant external factors, damped by overmolding.

The effect of varying power levels (Power Dissipation,  $P_D$ ), can be estimated. The following formulas represent the fundamental relationships used to estimate  $T_J$ , at  $P_D$ .

$$P_D = V_{IN} \times I_{IN} \quad (1)$$

$$\Delta T = P_D \times R_{\theta JA} \quad (2)$$

$$T_J = T_A + \Delta T \quad (3)$$

For example, given common conditions such as:  $T_A = 25^\circ\text{C}$ ,  $V_{CC} = 12\text{ V}$ ,  $I_{CC} = 9\text{ mA}$ , and  $R_{\theta JA} = 110\text{ }^\circ\text{C/W}$ , then:

$$P_D = V_{CC} \times I_{CC} = 12\text{ V} \times 9\text{ mA} = 108\text{ mW}$$

$$\Delta T = P_D \times R_{\theta JA} = 108\text{ mW} \times 110\text{ }^\circ\text{C/W} = 11.9^\circ\text{C}$$

$$T_J = T_A + \Delta T = 25^\circ\text{C} + 11.9^\circ\text{C} = 36.9^\circ\text{C}$$

A worst-case estimate,  $P_D(\max)$ , represents the maximum allowable power level ( $V_{CC}(\max)$ ,  $I_{CC}(\max)$ ), without exceeding  $T_J(\max)$ , at a selected  $R_{\theta JA}$  and  $T_A$ .

*Example:* Reliability for  $V_{CC}$  at  $T_A = 150^\circ\text{C}$ , package LH, using a low-K PCB.

Observe the worst-case ratings for the device, specifically:  $R_{\theta JA} = 110\text{ }^\circ\text{C/W}$ ,  $T_J(\max) = 165^\circ\text{C}$ ,  $V_{CC}(\max) = 24\text{ V}$ , and  $I_{CC}(\max) = 17\text{ mA}$ .

Calculate the maximum allowable power level,  $P_D(\max)$ . First, invert equation 3:

$$\Delta T_{\max} = T_J(\max) - T_A = 165^\circ\text{C} - 150^\circ\text{C} = 15^\circ\text{C}$$

This provides the allowable increase to  $T_J$  resulting from internal power dissipation. Then, invert equation 2:

$$P_D(\max) = \Delta T_{\max} \div R_{\theta JA} = 15^\circ\text{C} \div 110\text{ }^\circ\text{C/W} = 136\text{ mW}$$

Finally, invert equation 1 with respect to voltage:

$$V_{CC(\text{est})} = P_D(\max) \div I_{CC}(\max) = 136\text{ mW} \div 17\text{ mA} = 8\text{ V}$$

The result indicates that, at  $T_A$ , the application and device can dissipate adequate amounts of heat at voltages  $\leq V_{CC(\text{est})}$ .

Compare  $V_{CC(\text{est})}$  to  $V_{CC}(\max)$ . If  $V_{CC(\text{est})} \leq V_{CC}(\max)$ , then reliable operation between  $V_{CC(\text{est})}$  and  $V_{CC}(\max)$  requires enhanced  $R_{\theta JA}$ . If  $V_{CC(\text{est})} \geq V_{CC}(\max)$ , then operation between  $V_{CC(\text{est})}$  and  $V_{CC}(\max)$  is reliable under these conditions.

## Package Outline Drawings

### For Reference Only – Not for Tooling Use

(Reference DWG-2840)

Dimensions in millimeters – NOT TO SCALE

Dimensions exclusive of mold flash, gate burrs, and dambar protrusions  
Exact case and lead configuration at supplier discretion within limits shown

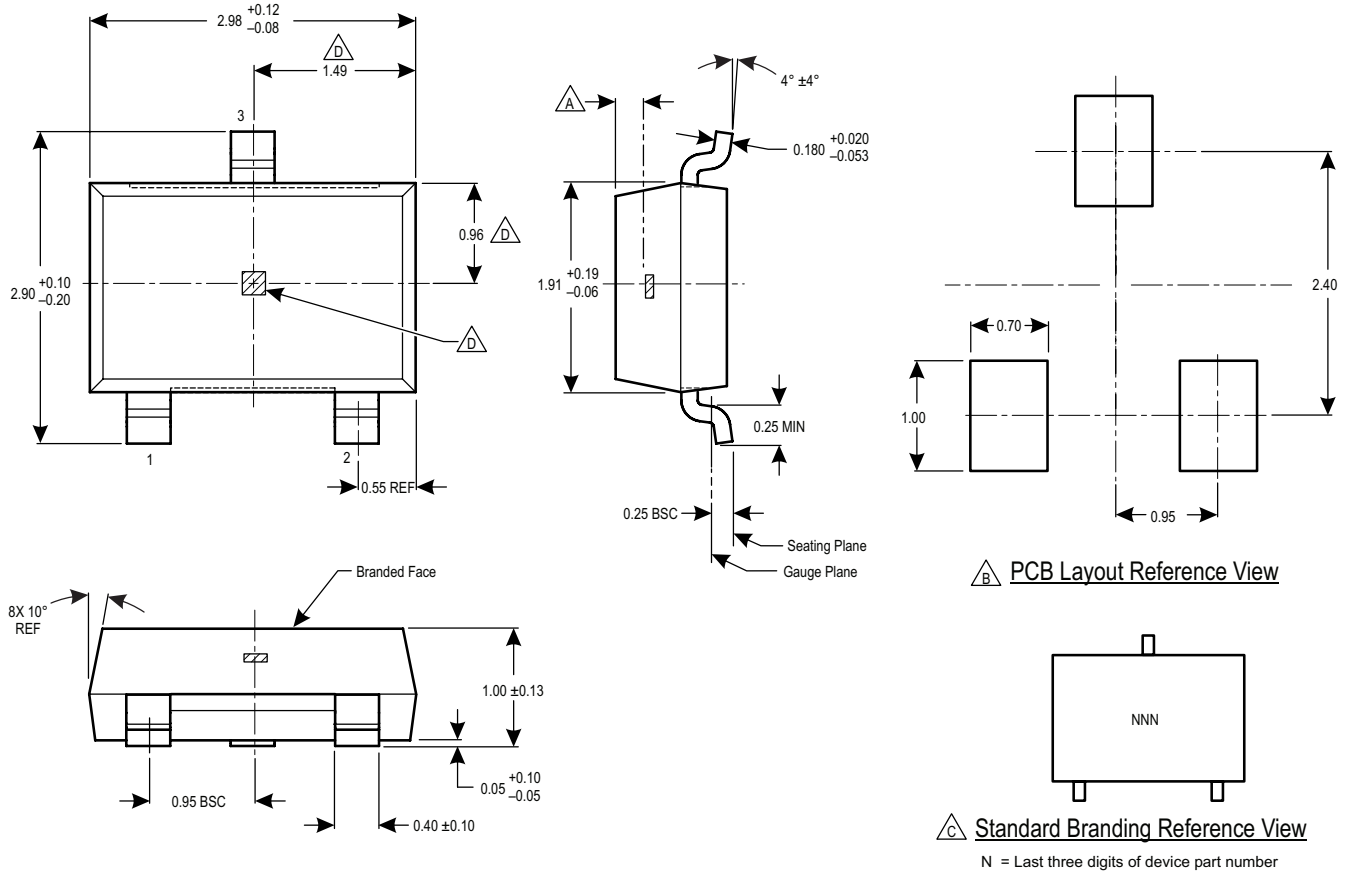


Figure 4: Package LH, 3-Pin SOT23W

For Reference Only – Not for Tooling Use

(Reference DWG-9013)  
Dimensions in millimeters – NOT TO SCALE  
Dimensions exclusive of mold flash, gate burrs, and dambar protrusions  
Exact case and lead configuration at supplier discretion within limits shown

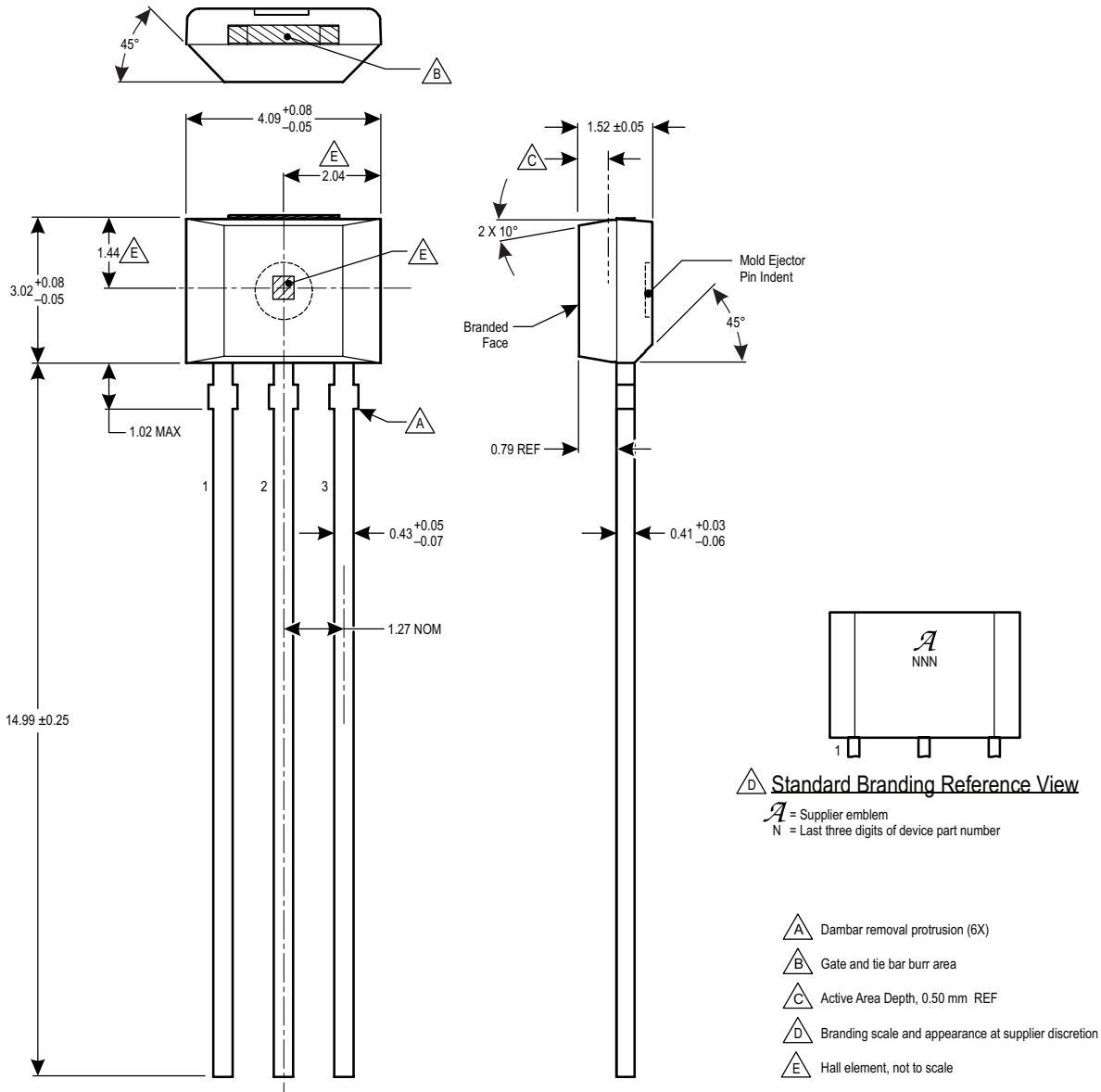


Figure 5: Package UA, 3-Pin SIP

**Revision History**

Revision	Date	Change
–	December 17, 2014	Initial Release
1	July 13, 2015	Corrected LH package Active Area Depth value

Copyright ©2013-15, Allegro MicroSystems, LLC

Allegro MicroSystems, LLC reserves the right to make, from time to time, such departures from the detail specifications as may be required to permit improvements in the performance, reliability, or manufacturability of its products. Before placing an order, the user is cautioned to verify that the information being relied upon is current.

Allegro's products are not to be used in any devices or systems, including but not limited to life support devices or systems, in which a failure of Allegro's product can reasonably be expected to cause bodily harm.

The information included herein is believed to be accurate and reliable. However, Allegro MicroSystems, LLC assumes no responsibility for its use; nor for any infringement of patents or other rights of third parties which may result from its use.

For the latest version of this document, visit our website:

[www.allegromicro.com](http://www.allegromicro.com)

